Gravitational Wave Signatures of the Accretion Disk-Induced Migration of a Small Black Hole Spiraling into a Supermassive Black Hole

Bence Kocsis,[1] Nicolás Yunes,[2,1] and Abraham Loeb[1]

[1] *Harvard-Smithsonian Center for Astrophysics, 60 Garden St., Cambridge, MA 02138, USA.*
[2] *Dept. of Physics and MIT Kavli Institute, 77 Massachusetts Avenue, Cambridge, MA 02139.*

(Dated: November 27, 2010)

We study the impact of spiral density waves on extreme mass-ratio inspirals embedded in a thin gaseous accretion disk. The interaction, analogous to Type-II planetary migration, modifies the phase evolution of the gravitational waves (GWs) and leads to phase differences of up to $\sim 10^4$ rads in a one-year observation. Frequency-domain waveforms in the stationary-phase approximation show that such effects are weakly-correlated with binary parameters. The measurement of disk parameters opens the possibility to use gravitational waves as probes of accretion disk physics.

Introduction. Gravitational waves (GWs) from extreme-mass ratio inspirals (EMRIs), a small compact object (SCOs) spiraling into a supermassive black hole (SMBHs), could be detected by the Laser Interferometer Space Antenna (LISA) [1]. Until recently, these EMRIs have been assumed to be isolated, as GWs were thought to be insensitive to the astrophysical environment. Recently, however, [2] showed that the presence of a secondary SMBH can lead to an observable Doppler-imprint on the EMRI signal even if the secondary is 0.1 pc away.

In this letter, we investigate another astrophysical imprint on EMRI GWs, that of radiatively-efficient, geometrically-thin, stationary accretion disks. Gas in orbit around the SMBH radiates thermally much faster than it can drift inward, thus forcing the disk to collapse into a thin geometry. Radiatively-efficient disks have the largest mass accretion rate and smallest drift velocity, making them the most massive. Inefficient disks around quiescent SMBHs are much less massive, dominated by different accretion flows (e.g. advection), and thus, leave a much weaker GW imprint [3].

We consider both Shakura-Sunyaev [4], α-disks, where the viscosity is proportional to the total (gas plus radiation) pressure, and β-disks [5], where the viscosity is proportional to the gas pressure only. α- and β-disks constitute the standard model of luminous active galactic nuclei (AGN). The main difference between them is that β-disks are more massive in the inner disk region relevant to LISA EMRIs, because the effective viscosity and radial inflow velocity are smaller. Due to the lack of a complete relativistic parameterization, we consider here Newtonian disk models only.

Numerical and observational experiments have not yet determined which of these is the correct disk model. Certain magnetohydrodynamic, accretion disk, numerical simulations support α-disks [6], while other simulations, where the diffusion scale is larger than the wavelength of the magneto-rotational instability, support β-disks [7, 8]. α-disks were thought to be viscously, thermally, and convectively linearly unstable [9–12], but simulations have found them to be thermally stable [13] and viscously unstable [14]. The instability in α-disks produces spectral variations that are not observed, while the β-disk model seems to better fit spectral data [15]. We here remain agnostic about the disk model, carrying out calculations for both of them.

EMRI formation scenarios that rely on accretion disks have been put forth [16, 17]. Stars may be captured or may form in accretion disks by fragmentation and/or coagulation of density enhancements; their remnants would be pushed inwards by the disk and could provide a reservoir of EMRI events in AGNs. This scenario, however, is not the dominant formation channel, with simple scattering being more likely [18]. Although EMRI rates are rather uncertain (between a few tens to a few hundreds over LISA's lifetime [19]), one might expect a few percent of these to be in AGN environments, implying rates of less than ~ 10 over LISA's lifetime.

Many accretion disk effects produce GW imprints, but we here focus on the dominant one: migration in the presence of a gap. As the SCO orbits, gravitational torques are generated by spiral density waves in the accretion disk. These torques transport angular momentum away from the binary, facilitating the SCO's migration, as in planetary dynamics [20]. Such a change in the angular momentum flux leaves a strong imprint in the GW spectrum. Other disk effects are subdominant, including the SMBH's or SCO's mass increase, modifications to the gravitational potential due to the disk's self-gravity and to the angular momentum flux due to hydrodynamic drag from gas winds.

Disk Properties. α- and β-disks are described by two free, disk parameters: the accretion rate $\dot{M}_\bullet$ and the α viscosity parameter. AGN observations suggest a relative accretion rate, $\dot{m}_\bullet \equiv \dot{M}_\bullet/\dot{M}_{\bullet\rm Edd} \in (0.1, 1)$, with a statistical increase towards higher luminosities [21, 22]. Evidence for the magnitude of α is inconclusive, with plausible theoretical ranges between $(0.01, 1)$ [23] and observational evidence for $(0.2, 0.4)$ [24, 25]. We here normalize parameters to $\dot{m}_{\bullet 1} = \epsilon_1 = \alpha_1 = 1$, where $A_n \equiv A/10^{-n}$. The disk surface density $\Sigma(r)$ and mid-plane height $H(r)$ for α- and β-disks can be found in Eqs. (4) and (5) of [26].

From these, one can easily construct the local disk mass $m_{\rm d} = 4\pi r^2\Sigma$, the disk volume density $\rho = \Sigma/(2H)$, the mean radial inflow velocity $v_r^{\rm gas} = -\dot{M}_\bullet r/m_{\rm d}$ and the isothermal sound speed $c_s = H\Omega$, where the gas' orbital velocity is $\Omega = (M_\bullet/r^3)^{1/2}$, with $M_\bullet$ the SMBH mass and r the orbital separation. Henceforth, $G = c = 1$.

A sufficiently massive SCO can open an annular gap in the disk because its gravitational torque pushes gas away faster than viscosity can replenish it [27–29]. For a gap to open, one of several criteria must be met: the SCO torque must exceed the viscous torque; the scale height must exceed the Hill radius or Roche lobe; and the gap width has to exceed the Hill radius. A gap then forms if the mass ratio $q \equiv m_\star/M_\bullet > q_{\rm gap}$, where

$$q_{\rm gap} \equiv \max\left\{\frac{81}{64}\frac{H^3}{r^3}, \sqrt{40\alpha}\,\beta^{b/2}\frac{H^{5/2}}{r^{5/2}}, 50\alpha\beta^b\frac{H^2}{r^2}\right\}\,, \quad (1)$$

and where $m_\star$ is the SCO's mass, $b = 0$ or 1 for α- and β-disks and β is the ratio of the gas to total pressure (see Eq. (3) in [26]). One can invert this relation to find a minimum radius outside which a gap forms. In general, a gap is likely to open if the SCO is captured by the accretion disk at large radius $r/M_\bullet \gg 50$. As the SCO drifts inwards, it will eventually cross the radius where the gap will start to refill $r/M_\bullet \sim 35$, but this gap will not close immediately, as the diffusion and inspiral times are comparable at this radii for β-disks.

Migration. Whether a gap opens or not, the orbiting SCO exerts a non-zero average gravitational torque on the disk, generating a spiral density wave that transports angular momentum away. This torque can exchange angular momentum resonantly with the SCO, facilitating its *migration* [27] as in planetary dynamics [20]. Type-II migration occurs in the presence of a gap [30, 31]. For LISA EMRIs, "secondary dominated Type-II migration" is relevant because the local disk mass is smaller than the SCO's. We here employ both the model of [30] (Type-IIa), where angular momentum exchange is assumed to be dominated by processes in the inner-edge of the disk and accretion is not significantly quenched across the gap, and the model of [31], where the steady-state assumption is relaxed with zero-stress boundary conditions at the SCO and gap quenching. A third type of migration is possible in planetary dynamics, but this is irrelevant for LISA EMRIs.

For Type IIa migration, the modification to the flux of specific angular momentum is [30]

$$\dot{\ell}_{\rm IIa} = -\left(\frac{m_{\rm d}}{m_\star}\right)^k \frac{v_{\rm orb}v_r^{\rm gas}}{2} \quad (2)$$

where $v_{\rm orb} = (M_\bullet/r)^{1/2}$ is the azimuthal orbital velocity and $k = 3/8$ for electron-scattering opacity and β-disks. Neglecting the banking up of gas near the outer edge of the gap, angular momentum balance implies $k = 1$, which we adopt conservatively for α-disks. Relative to the GW flux of specific angular momentum,

$$\frac{\dot{\ell}_{\rm IIa}}{\dot{\ell}_{\rm GW}} = \begin{cases} 6.2\times10^{-6}\,\dot{m}_{\bullet 1}M_{\bullet 5}^3 m_{\star 1}^{-2}\bar{r}_{10}^4\,, & \text{for } \alpha\,, \\ 7.6\times10^{-3}\,\alpha_1^{1/2}\dot{m}_{\bullet 1}^{5/8}M_{\bullet 5}^{13/8}m_\star^{-11/8}\bar{r}_{10}^{25/8}\,, & \text{for } \beta\,. \end{cases} \quad (3)$$

For Type IIb migration, the flux of specific angular momentum is [31]

$$\dot{\ell}_{\rm IIb}^\beta = -c_2 v_{\rm orb}\frac{\dot{M}_\bullet}{m_\star}(r\,r_{\rm d})^{1/2}\,, \quad (4)$$

where $r_{\rm d}$ satisfies $m_{\rm d}(r_{\rm d}) = m_\star$, $c_2 \equiv \{1+\delta[1-(r/r_{\rm d})^{1/2}]\}^{k_2}$, $\delta = 6.1$, and $k_2 = 0.26$. For $r = r_d$, $c_2 = 1$ so both Type IIa and b migration imply a migration rate that tracks the radial velocity of gas. Relative to the GW flux,

$$\frac{\dot{\ell}_{\rm IIb}^\beta}{\dot{\ell}_{\rm GW}} = 6.0\times10^{-4}\,\alpha_1^{2/7}\dot{m}_{\bullet 1}^{11/14}M_{\bullet 5}^{31/14}m_{\star 1}^{-23/14}\bar{r}_{10}^{7/2}\,, \quad (5)$$

where Type IIb migration is valid only for β-disks.

Type II migration can be quenched if the SCO's evolution decouples from the gap. When the orbital separation is small enough, the GW inspiral velocity can overtake the viscous inflow rate and the gap will not be able to keep up with the SCO [32]. This occurs inside the transition radius

$$\bar{r}_{\rm tr} = \begin{cases} 1.2\times10^{-4}\,\alpha_1^{-2}\dot{m}_{\bullet 1}^{-4}M_{\bullet 5}^{-2}m_{\star 1}^2\lambda^5\,, & \text{for } \alpha \\ 13\,m_{\star 1}^{5/13}\alpha_1^{-4/13}\dot{m}_{\bullet 1}^{-2/13}M_{\bullet 5}^{-4/13}m_{\star 1}^{5/13}\lambda^{2/13}\,, & \text{for } \beta \end{cases} \quad (6)$$

where λr is the gap radius (we choose $\lambda = 1.7$). If the SCO and disk decouple, disk torques will shift out of resonance and become too distant for efficient angular momentum exchange. We conservatively assume that Type II migration shuts off completely inside $r \le r_{\rm tr}$ and we neglect torques from the gas interior to the SCO.

GW Implications. The change in the angular momentum dissipation rate due to migration modifies the GW evolution. One can see this simply from the evolution equation of the orbital frequency $\dot{F} = \dot{L}\,(dL/dF)^{-1}$, where now $\dot{L} \to \dot{L}_{\rm GW}(1+\delta\dot{\ell}/\dot{\ell}_{\rm GW})$, with $\delta\dot{\ell}$ any of Eqs. (2) or (4). Integrating the orbital frequency twice, the difference in the phase of the dominant GW mode (relative to the vacuum expectation) is simply

$$\delta\phi_{\rm GW} = A_1\alpha_1^{a_1}m_{\star 1}^{a_2}\dot{m}_{\bullet 1}^{a_3}M_{\bullet 5}^{a_4}r_{0,20}^{a_5}\left[1 + A_2x^{a_5} - (A_2+1)\,x^{a_6}\right]\,, \quad (7)$$

where $x \equiv r_f/r_0$ is the ratio of final to initial EMRI separations and $r_{0,20} \equiv r_0/(20M_\bullet)$ is the normalized, initial radius. Details of this calculation will be presented elsewhere. The parameters (A_i, a_i) depend on the type of migration and are given in Table I. Notice that $a_5 > 0$ since disk effects become larger at larger radii.

Figure 1 plots the phase differences of Eq. (7) for a one year EMRI. The solid, dotted and dot-dashed curves

	A_1	A_2	a_1	a_2	a_3	a_4	a_5	a_6
IIa, α	-10^{-2}	$-16/3$	0	-3	1	4	13/2	8
IIa, β	-29	$-19/4$	1/2	$-19/8$	5/8	21/8	45/8	57/8
IIb, β	-1.4	-5	2/7	$-37/14$	11/14	45/14	6	15/2

TABLE I. Columns are parameters in Eq. (7) and rows are migration effects.

correspond to α-disk, Type IIa migration, β-disk Type IIa migration and β-disk Type IIb migration respectively. The top and bottom panel correspond to EMRIs with different SMBH masses. For comparison, we also plot the total GW phase accumulation in thin, solid magenta, and a rough measure of LISA's accuracy to phase measurements: $\delta\phi_{\rm GW} > 10/\rho$, with ρ computed at 1 Gpc (thick solid magenta) and at 10 Mpc (thick dashed magenta). Observe that the blue lines are always above the accuracy requirements for EMRIs orbiting inside $10M$.

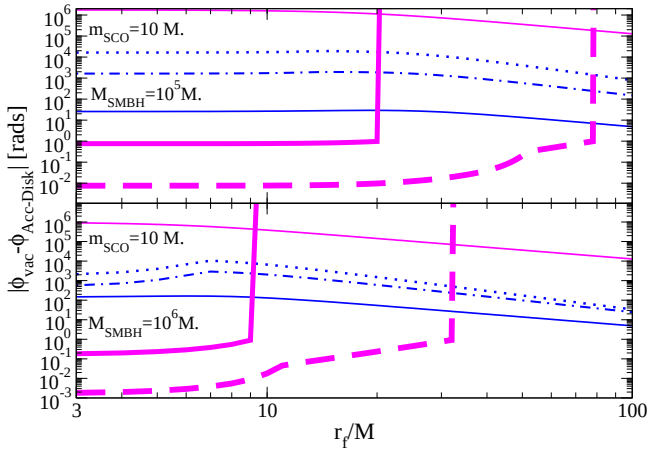

FIG. 1. Phase difference between vacuum and non-vacuum GWs as a function of final radius for a 1 year evolution.

One might worry that the above estimates are flawed due to the use of a Newtonian waveform model to describe gravitational radiation. This worry is put at easy in Fig. 2, where we plot similar phase differences, but using the relativistic, calibrated effective-one-body, waveform model of [33–35] (for a SMBH with spin $a_\bullet/M_\bullet = 0.9$) and after first aligning the waveforms in time and phase, a procedure that maximizes the overlap between waveforms. This figure follows the same curve coding as Fig. 1. Observe that differences induced by Type-II migration easily exceed a 1 radian threshold within 2 weeks (β-disks) and 2 months (α-disks). For Type I migration, only the effect of β-disks would be visible in observations that last less than a 1 year.

The dephasing estimates presented above do not properly account for the intrinsic noise in the detector. Figure 3 shows the mismatch between vacuum and non-vacuum waveforms as a function of time, after mini-

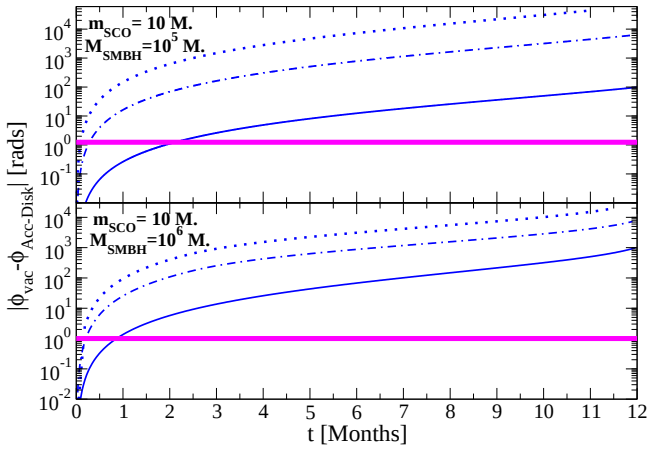

FIG. 2. Aligned phase difference between vacuum and non-vacuum GWs as a function of time.

maximization over time and phase. For a definition of the mismatch, see eg. Eq. (32) in [35]. A mismatch over 3% indicates that waveforms are sufficiently different that a data analysis search with templates placed at such mismatches would be able to distinguish them. The decrease

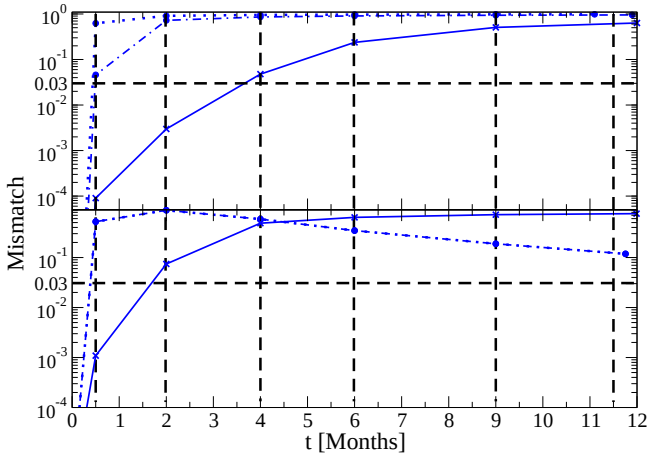

FIG. 3. Mismatch between vacuum and non-vacuum GWs as a function of time after mini-maximization [35].

in mismatch after 2 months is due to the fact that Type II migration is quenched by decoupling at that stage of the evolution onwards for the more massive system.

A large absolute phase difference or mismatch, however, does not guarantee that accretion disk parameters could be faithfully extracted given an EMRI detection. This is because accretion disk modifications to the waveform templates might be degenerate with standard EMRI system parameters. We have calculated the Fourier transform of Newtonian waveforms in the stationary-phase approximation and found that the frequency-domain phase is

$$\psi/\psi_{\rm vac} = 1 - \tilde{A}_1 \alpha_1^{\tilde{a}_1} \dot{m}_{\bullet 1}^{\tilde{a}_2} M_{\bullet 5}^{\tilde{a}_3} q_0^{\tilde{a}_4} u_0^{\tilde{a}_5}\,, \qquad (8)$$

where $q_0 \equiv q/10^{-4}$ is the normalized mass ratio and $u_0 \equiv (\pi \mathcal{M} f)/(6.15 \times 10^{-5})$ is a normalized reduced frequency, with $\mathcal{M} = q^{3/5} M_\bullet$ the chirp mass and a GW frequency of 10^{-2} Hz. The vacuum frequency-domain phase is $\psi_{\rm vac} = (3/128) u^{-5/3}$ and the parameters $(\tilde{A}_i, \tilde{a}_i)$ are given in Table II.

	$\tilde{A}_1$	$\tilde{a}_1$	$\tilde{a}_2$	$\tilde{a}_3$	$\tilde{a}_4$	$\tilde{a}_5$
IIa, α	-10^{-5}	0	1	1	$-2/5$	$-8/3$
IIa, β	-10^{-2}	$1/2$	$5/8$	$1/4$	$-1/8$	$-25/12$
IIb, β	-10^{-3}	$2/7$	$11/14$	$4/7$	$-17/70$	$-7/3$

TABLE II. Columns are parameters in Eq. (8) and rows are migration effects.

Notice that the frequency exponent $a_5 < 0$, implying it is dominant over the Newtonian term at low frequencies (large radii). Because of this, no term in a post-Newtonian expansion can ever become 100% degenerate with corrections of the form of Eq. (8). We thus conclude that accretion disk effects are weakly correlated with standard EMRI parameters.

Discussion. If there is an accretion disk imprint in EMRI GWs, then their detection could inform us about disk physics, allowing measurements of disk parameters to better than 10%, at the cost of complicating the waveform modeling. If so, they could provide candidates for electromagnetic counterpart searches. For example, a GW measurement of the accretion rate parameter would imply a plausible range of AGN luminosities, which when combined with the LISA source location estimate ($\sim 1^\circ$ angular, $\sim 10^{-3}$ fractional distance [36]), might allow telescopes to find the right AGN, as these are relatively sparsely distributed. This would allow EMRIs to serve as standard sirens to independently test cosmological models [37]. Peculiar velocities and weak lensing errors could thus be alleviated through the inclusion of low redshift, EMRI events [38].

In this letter, we have made several approximations to allow for a first-study of this problem. Topics of future study include EMRIs in more generic orbits and modeling of relativistic accretion disks. In a forthcoming publication, we will present much more detail, together with a more thorough study of other accretion disk effects.

Acknowledgments. BK and NY acknowledge support from the NASA through Einstein Postdoctoral Fellowship Award Number PF9-00063 and PF0-110080 issued by the Chandra X-ray Observatory Center, operated by the Smithsonian Astrophysical Observatory for and on behalf of NASA under contract NAS8-03060. BK acknowledges partial support from OTKA grant 68228 and AL from NSF grant AST-0907890 and NASA grants NNX08AL43G and NNA09DB30A.

[1] K. Danzmann and A. Rüdiger, Class. Quantum Grav. **20**, S1 (2003).
[2] N. Yunes, M. Miller, and J. Thornburg, (2010), * Temporary entry *, arXiv:arXiv:1010.1721 [astro-ph.GA].
[3] R. Narayan, The Astrophysical Journal **536**, 663 (2000), arXiv:astro-ph/9907328.
[4] N. I. Shakura and R. A. Sunyaev, Astron. Astroph. **24**, 337 (1973).
[5] P. J. Sakimoto and F. V. Coroniti, ApJ **247**, 19 (1981).
[6] K. Ohsuga, S. Mineshige, M. Mori, and Y. Kato, PASJ **61**, L7+ (2009), arXiv:0903.5364 [astro-ph.HE].
[7] N. J. Turner, J. M. Stone, J. H. Krolik, and T. Sano, ApJ **593**, 992 (2003), arXiv:astro-ph/0304511.
[8] N. J. Turner, ApJ **605**, L45 (2004), arXiv:astro-ph/0402539.
[9] A. P. Lightman and D. M. Eardley, ApJ **187**, L1+ (1974).
[10] N. I. Shakura and R. A. Sunyaev, MNRAS **175**, 613 (1976).
[11] G. S. Bisnovatyi-Kogan and S. I. Blinnikov, A&A **59**, 111 (1977).
[12] T. Piran, ApJ **221**, 652 (1978).
[13] S. Hirose, J. H. Krolik, and O. Blaes, ApJ **691**, 16 (2009), arXiv:0809.1708.
[14] S. Hirose, O. Blaes, and J. H. Krolik, ApJ **704**, 781 (2009), arXiv:0908.1117 [astro-ph.HE].
[15] C. Done and S. W. Davis, ApJ **683**, 389 (2008), arXiv:0803.0584.
[16] J. Goodman and J. C. Tan, ApJ **608**, 108 (2004), arXiv:astro-ph/0307361.
[17] Y. Levin, Mon. Not. Roy. Astron. Soc. **374**, 515 (2007), arXiv:astro-ph/0603583.
[18] P. Amaro-Seoane, J. R. Gair, M. Freitag, M. C. Miller, I. Mandel, C. J. Cutler, and S. Babak, Classical and Quantum Gravity **24**, 113 (2007), arXiv:astro-ph/0703495.
[19] J. R. Gair, Class. Quant. Grav. **26**, 094034 (2009), arXiv:0811.0188 [gr-qc].
[20] P. J. Armitage, ArXiv Astrophysics e-prints (2007), arXiv:astro-ph/0701485.
[21] J. A. Kollmeier, C. A. Onken, C. S. Kochanek, A. Gould, D. H. Weinberg, M. Dietrich, R. Cool, A. Dey, D. J. Eisenstein, B. T. Jannuzi, E. Le Floc'h, and D. Stern, ApJ **648**, 128 (2006), arXiv:astro-ph/0508657.
[22] J. R. Trump, C. D. Impey, B. C. Kelly, M. Elvis, A. Merloni, A. Bongiorno, J. Gabor, H. Hao, P. J. McCarthy, J. P. Huchra, M. Brusa, N. Cappelluti, A. Koekemoer, T. Nagao, M. Salvato, and N. Z. Scoville, ApJ **700**, 49 (2009), arXiv:0905.1123 [astro-ph.CO].
[23] M. E. Pessah, C. Chan, and D. Psaltis, ApJ **668**, L51 (2007), arXiv:0705.0352.
[24] G. Dubus, J. Hameury, and J. Lasota, A&A **373**, 251 (2001), arXiv:astro-ph/0102237.
[25] A. R. King, J. E. Pringle, and M. Livio, MNRAS **376**, 1740 (2007), arXiv:astro-ph/0701803.
[26] Z. Haiman, B. Kocsis, and K. Menou, ApJ **700**, 1952 (2009), arXiv:0904.1383 [astro-ph.CO].
[27] P. Goldreich and S. Tremaine, ApJ **241**, 425 (1980).
[28] D. N. C. Lin and J. Papaloizou, ApJ **309**, 846 (1986).
[29] P. Artymowicz and S. H. Lubow, ApJ **421**, 651 (1994).
[30] D. Syer and C. J. Clarke, MNRAS **277**, 758 (1995),

arXiv:astro-ph/9505021.
[31] P. B. Ivanov, J. C. B. Papaloizou, and A. G. Polnarev, MNRAS **307**, 79 (1999), arXiv:astro-ph/9812198.
[32] M. Milosavljević and E. S. Phinney, ApJ **622**, L93 (2005), arXiv:astro-ph/0410343.
[33] N. Yunes, A. Buonanno, S. A. Hughes, M. Coleman Miller, and Y. Pan, Phys.Rev.Lett. **104**, 091102 (2010), arXiv:arXiv:0909.4263 [gr-qc].
[34] N. Yunes, GW Notes, Vol. 2, p. 3-47 **2**, 3 (2009).
[35] N. Yunes, A. Buonanno, S. A. Hughes, Y. Pan, E. Barausse, *et al.*, (2010), * Temporary entry *, arXiv:arXiv:1009.6013 [gr-qc].
[36] L. Barack and C. Cutler, Phys. Rev. **D69**, 082005 (2004), arXiv:gr-qc/0310125.
[37] D. E. Holz and S. A. Hughes, ApJ **629**, 15 (2005), arXiv:astro-ph/0504616.
[38] B. Kocsis, Z. Frei, Z. Haiman, and K. Menou, ApJ **637**, 27 (2006), arXiv:astro-ph/0505394.